Legendre Analysis of Differential Distributions in Hadronic Reactions

Yakov I. Azimov,[1,*] Igor I. Strakovsky,[2,†] William J. Briscoe,[2] and Ron L. Workman[2]

[1] *Petersburg Nuclear Physics Institute, NRC Kurchatov Institute, Gatchina, 188300, Russia*
[2] *The George Washington University, Washington, DC 20052, USA*

(Dated: January 3, 2017)

Abstract

Modern experimental facilities, such as CBELSA, ELPH, JLab, MAMI and SPring-8 have provided a tremendous volume of data, often with wide energy and angular coverage, and with increasing precision. For reactions with two hadrons in the final state, these data are often presented as multiple sets of panels, with angular distributions at numerous specific energies. Such presentations have limited visual appeal, and their physical content is typically extracted through some model-dependent treatment. Instead, we explore the use of a Legendre series expansion with a relatively small number of essential coefficients. This approach has been applied in several recent experimental investigations. We present some general properties of the Legendre coefficients in the helicity framework and consider what physical information can be extracted without any model-dependent assumptions.

arXiv:1701.00124v1 [hep-ph] 31 Dec 2016

* Deceased.
† igor@gwu.edu; Corresponding author.

I. INTRODUCTION

Modern detectors, combined with the present generation of accelerator facilities, are capable of providing large reaction-specific sets of experimental data. These sets have often been combined in partial-wave analyses with the hope of extracting elements of the fundamental reaction process (such as resonance parameters and coupling constants). The analyses generally have some model-dependence and are limited by the quality of the available data.

Here we address the problem of displaying these large data sets, evaluating their physical content, and determining their sensitivity to partial-wave content in a model-independent manner. Even in relatively simple cases of $2 \to 2$ reactions, data are usually presented as multi-panel pictures with a great number of angular distributions for different energies (and/or energy distributions for different angles). Such an approach can be used, of course, to compare with various models, but is not practical for any direct extraction of physical information.

In several recent works, we and others have suggested and applied another approach, involving the expansion of differential cross sections, for both unpolarized [1, 2] and polarized [3] photoproduction of single pseudoscalar mesons, in terms of Legendre coefficients. For a limited energy interval, it appears sufficient to use a finite number of the expansion terms, which may be plotted as a function of energy, thus providing a more clear and visually suggestive presentation, which may be further analyzed through models or partial-wave analyses.

Preliminary results of this study were reported at the *Hadron Structure and QCD: from Low to High Energies* Workshop [4]. In the present paper, we further describe and study this approach more systematically. Then we discuss its utility for the extraction of model-independent information.

II. EXPANSION OF AMPLITUDES AND CROSS SECTIONS

Let us consider $2 \to 2$ reaction

$$a + b \to c + d\,, \tag{1}$$

where particles have spins s_a, s_b, s_c, s_d. It can be described by helicity amplitudes [5] $A_{\lambda_c\lambda_d;\,\lambda_a\lambda_b}(W,z,\phi)$, where λ_a, λ_b, λ_c, and λ_d are the corresponding s-channel helicities, W is the center-of-mass (c.m.) energy, and $z = \cos\theta$. The angles θ and ϕ are, respectively, the polar and azimuthal c.m. angles. These amplitudes may be decomposed in terms of the Wigner harmonics

$$A_{\lambda_c\lambda_d;\,\lambda_a\lambda_b}(W,z,\phi) = F_{\lambda_c\lambda_d;\,\lambda_a\lambda_b}(W,z)\, e^{i(\lambda-\mu)\phi} \tag{2}$$

$$= \sum_j (2j+1)\, f^j_{\lambda_c\lambda_d;\,\lambda_a\lambda_b}(W)\, d^j_{\lambda\mu}(z)\, e^{i(\lambda-\mu)\phi} \tag{3}$$

with partial-wave amplitudes

$$f^j_{\lambda_c\lambda_d;\,\lambda_a\lambda_b}(W) = \frac{1}{p}\,\langle\lambda_c\lambda_d|T^j(W)|\lambda_a\lambda_b\rangle\ , \tag{4}$$

being elements of the T-matrix, related to the S-matrix, $T = (S-1)/(2i)$, p being the initial relative c.m. momentum, and

$$\lambda = \lambda_a - \lambda_b\,, \qquad \mu = \lambda_c - \lambda_d\,. \tag{5}$$

The scattering/production angle θ is taken to be the angle between the c.m. momenta of particles c and a (or d and b). All the values of j, λ, μ are simultaneously either integer or half-integer and the above j-summation runs over all physical values of $j \geq |\lambda|, |\mu|$.

The differential cross section, with all initial and final helicities fixed, is [5]

$$d\sigma_{\lambda_c\lambda_d;\,\lambda_a\lambda_b} = \left(\frac{2\pi}{p}\right)^2 |A_{\lambda_c\lambda_d;\,\lambda_a\lambda_b}(W,z,\phi)|^2\ d\Omega\,. \tag{6}$$

Note that $d\sigma/d\Omega$ is independent of the azimuthal angle ϕ, since every particular helicity amplitude depends on ϕ only through a phase factor.

The totally unpolarized differential cross section can be written as

$$\frac{d\sigma(W,z)}{dz} = N \sum_{(\lambda,\mu)} |F_{\lambda_c\lambda_d;\,\lambda_a\lambda_b}(W,z)|^2 \tag{7}$$

$$= N \sum_{(\lambda,\mu)} \sum_{j_1,j_2} (2j_1+1)(2j_2+1)\, f^{j_1\,*}_{\lambda_c\lambda_d;\,\lambda_a\lambda_b}(W)\, f^{j_2}_{\lambda_c\lambda_d;\,\lambda_a\lambda_b}(W)\, d^{j_1}_{\lambda\mu}(z)\, d^{j_2}_{\lambda\mu}(z)\,, \tag{8}$$

where $\sum_{(\lambda,\mu)}$ implies summation over all initial and final helicities. We separate out the normalization factor N, which has a simple structure, with a known dependence on the energy and on the spins (due to summing and averaging over polarization states), but is quite independent of any dynamics, helicities, angles, and angular momenta (it is not essential for the following discussion). The angular dependence of each summand in Eq.(8) is completely described by two d-harmonics with the same λ and μ. Their product can be decomposed into a Clebsch-Gordan series over the Legendre polynomials. As a result, we obtain

$$\frac{d\sigma(W,z)}{dz} = \sum_{J=0}^{\infty} A_J^{(\sigma)}(W)\, P_J(z) \tag{9}$$

with integer J. According to the composition rules for angular momenta, every $A_J^{(\sigma)}(W)$ contains bilinear contributions of partial-wave amplitudes (see Eq.(8)) with angular momenta j_1 and j_2 satisfying the familiar relations

$$|j_1 - j_2| \le J \le j_1 + j_2\,. \tag{10}$$

This means that a particular Legendre coefficient $A_J^{(\sigma)}(W)$ generally contains an infinite number of contributions from partial-wave amplitudes with various j-values. But it evidently can not contain interference of amplitudes with too different j_1 and j_2 (*i.e.*, with $|j_1 - j_2| > J$). Quadratic terms, having $j_1 = j_2 = j$, may appear only at sufficiently large $j \ge J/2$. Of course, the coefficient $A_0^{(\sigma)}(W)$ coincides with half the total cross section of reaction (1) at the energy W. Recall that $\sigma^{\rm tot} = 4\pi A_0^{(\sigma)}$ if one fits $d\sigma/d\Omega$.

The Legendre coefficients have another, less evident, property. To derive it, we combine Eqs.(A1), (A2), and (41) of Ref. [5] and obtain

$$d^j_{\lambda\mu}(-z)\,\langle\lambda_c\lambda_d|T^j(W)\,|\lambda_a\lambda_b\rangle = \frac{(-1)^{s_a+s_b-\mu}}{\eta_a\eta_b}\, d^j_{\lambda'\mu}(z)\,\langle\lambda_c\lambda_d|T^j(W)\,P|\lambda'_a\lambda'_b\rangle\,, \tag{11}$$

$$F_{\lambda_c\lambda_d;\,\lambda_a\lambda_b}(W,-z) = \frac{(-1)^{s_a+s_b-\mu}}{\eta_a\eta_b}\, F^{(P)}_{\lambda_c\lambda_d;\,\lambda'_a\lambda'_b}(W,z)\,. \tag{12}$$

Here $\lambda'_a = -\lambda_a$, $\lambda'_b = -\lambda_b$, $\lambda' = -\lambda$, η_a and η_b are the internal parities of the particles a and b; P is the space reflection operator. The amplitudes $F^{(P)}(W,z)$ have the same structure as $F(W,z)$ (see Eq.(3)), but the partial-wave amplitudes are taken with the space-reflected initial states. The first factor in the right-hand side of Eqs.(11) and (12) is independent of j and, when squared, is always unity, since $(s_a + s_b - \mu)$ is always an integer. Of course, these relations could be rewritten in a different form, with space reflection affecting the final (instead of initial) states.

Now we can write the differential cross section in two forms:

$$\frac{d\sigma(W,-z)}{dz} = \sum_{J=0}^{\infty} A_J^{(\sigma)}(W)\, P_J(-z) = \sum_{J=0}^{\infty} A_J^{(\sigma,\,P)}(W)\, P_J(z)\,, \tag{13}$$

where $A_J^{(\sigma,\,P)}(W)$ has the same structure as $A_J^{(\sigma)}(W)$, but helicity summation uses space-reflected initial (or final) states. Since $P_J(-z) = (-1)^J P_J(z)$, we derive

$$A_J^{(\sigma,\,P)}(W) = (-1)^J\, A_J^{(\sigma)}(W)\,. \tag{14}$$

If the states used in the summation are separated by their parities, then this equality means that $A_J^{(\sigma)}$-coefficients with odd J-values may contain only contributions which are bilinear in states of opposite parities. For even J, on the other hand, bilinear contributions also appear in the $A_J^{(\sigma)}$, but only with both states of the same parity, positive or negative. Quadratic contributions of any state can appear only at even J. This means, in particular, that proper Breit-Wigner (BW) contributions of a resonance of an integer spin j_R appear in the even-J Legendre coefficients with $0 \le J \le 2j_R$. But if the spin is half-integer, these BW contributions do not appear at $J = 2j_R$; they appear only at even J with $0 \le J \le 2j_R - 1$.

The above expressions clearly demonstrate the well-known statement that the unpolarized cross section by itself does not allow a determination of the parity of a particular partial wave, since simultaneous reversal of parities for *all* partial waves does not influence the cross section. However, if there is a resonance with known quantum numbers, including its parity, then such complete parity reversal becomes impossible, and even unpolarized cross section is able to provide some information on partial-wave parities. Below we will discuss this point in more detail.

Described above is the Legendre decomposition for the unpolarized differential cross sections. However, such an approach may be applied also to processes with polarized particles and/or to polarization observables (more exactly, to polarization observables multiplied by the unpolarized differential cross section). Such quantities may kinematically vanish at $z = \pm 1$ (they may even have square root singularities there). Decomposition in Legendre polynomials then becomes inadequate, and one should instead use Wigner harmonics (or, in particular, associated Legendre polynomials) with integer J. For example, the beam asymmetry studied by the CLAS Collaboration [3] contains the kinematical factor $(1-z^2)$ which automatically arises in any converging series over the associated Legendre polynomials $P_J^2(z)$). In such cases the decomposition retains connection (10) between J and j_1, j_2; relation (11) again allows one to separate interferences of states with the same or with opposite parities.

Let us briefly discuss one more point. The series (3) and (9) generally sum an infinite number of terms. In practical cases, the series will be truncated. This may be justified on the basis of physical reasons (*e.g.*, presence of pronounced resonances in the data, with known definite spins and parities) or phenomenological ones (*e.g.*, higher Legendre coefficient may be safely discarded if their fitting errors exceed fitted values). In both cases, we obtain a limited number of parameters to describe experimental data and to investigate their physical content.

III. PHOTOPRODUCTION OF A SPINLESS MESON

To illustrate the above approach, we consider in more detail the particular case of a pseudoscalar-meson photoproduction off the proton, for instance,

$$\gamma + p \to \pi^+ + n\,. \tag{15}$$

The initial state has four possible helicity combinations ($\lambda_\gamma = \pm 1$, $\lambda_p = \pm 1/2$), while the final state has two helicity combinations ($\lambda_\pi = 0$, $\lambda_n = \pm 1/2$). Thus, there are eight different transitions between various initial and final helicities and, generally, eight different helicity amplitudes.

It is interesting to emphasize that the value of λ unambiguously determines all initial helicities: if $\lambda = \pm 1/2$, then $\lambda_\gamma = \pm 1$, $\lambda_p = \pm 1/2$; if $\lambda = \pm 3/2$, then $\lambda_\gamma = \pm 1$, $\lambda_p = \mp 1/2$ (of course, this is due to absence of $\lambda_\gamma = 0$). Hence, the independent amplitudes may be denoted as $F_{\lambda\pm}(W,z)$, where the sign in the index is the sign of μ, opposite to the sign of helicity of the final nucleon. Expression (8) for the unpolarized cross section may be rewritten as

$$\frac{d\sigma(W,z)}{dz} = N \sum_\lambda \left[|F_{\lambda+}(W,z)|^2 + |F_{\lambda-}(W,z)|^2 \right] \tag{16}$$

with λ-summation over four values $\pm 1/2, \pm 3/2$. The initial state with a particular value of λ can be realized by using the circularly polarized photon (with a definite helicity) together with the longitudinally polarized target nucleon. Therefore, also measurable is the cross section for any fixed λ:

$$\frac{d\sigma^{(\lambda)}(W,z)}{dz} = 4N \left[|F_{\lambda+}(W,z)|^2 + |F_{\lambda-}(W,z)|^2 \right] . \tag{17}$$

The additional factor 4, as compared to Eq.(16), arises since $d\sigma^{(\lambda)}/dz$ deals with a single initial state, while the unpolarized expression (16) implies averaging over four initial states with different helicities.

Note that amplitudes with all helicities reversed are related by parity conservation [5], so that only four of the eight amplitudes are independent. Eq.(44) of Ref. [5], applied to the photoproduction reaction, gives

$$F_{-\lambda\pm}(W,z) = (-1)^{\lambda \mp 1/2}\, F_{\lambda\mp}(W,z)\,. \tag{18}$$

Therefore, we can use only amplitudes with positive values of $\lambda = 1/2,\, 3/2$. For negative values of λ we have

$$F_{-1/2\pm}(W,z) = \pm F_{1/2\mp}(W,z)\,, \quad F_{-3/2\pm}(W,z) = \mp F_{3/2\mp}(W,z)\,.$$

As a result,

$$\frac{d\sigma^{(-1/2)}(W,z)}{dz} = \frac{d\sigma^{(1/2)}(W,z)}{dz}\,, \qquad \frac{d\sigma^{(-3/2)}(W,z)}{dz} = \frac{d\sigma^{(3/2)}(W,z)}{dz}$$

due to parity conservation. Moreover,

$$\frac{d\sigma(W,z)}{dz} = \frac{1}{2}\left[\frac{d\sigma^{(1/2)}(W,z)}{dz} + \frac{d\sigma^{(3/2)}(W,z)}{dz} \right] . \tag{19}$$

Difference of the helicity cross sections is related to the double polarization observable E:

$$\check{E}(W,z) = E \cdot \frac{d\sigma(W,z)}{dz} = \frac{1}{2}\left[\frac{d\sigma^{(1/2)}(W,z)}{dz} - \frac{d\sigma^{(3/2)}(W,z)}{dz}\right] . \tag{20}$$

Following Walker [6], if we let H_1 to H_4 label the four independent helicity amplitudes, the translation to amplitudes of the form $A_{\mu\lambda}(W,z,)$ is given in Table I.

TABLE I. Walker notation [6] for helicity amplitudes $A_{\mu\lambda}(W,z)$.

$\lambda\to$	$\lambda_\gamma=+1$		$\lambda_\gamma=-1$	
$\mu\downarrow$	$\frac{3}{2}$	$\frac{1}{2}$	$-\frac{1}{2}$	$-\frac{3}{2}$
$\frac{1}{2}$	H_1	H_2	H_4	-H_3
$-\frac{1}{2}$	H_3	H_4	-H_2	H_1

Partial-wave decomposition of the amplitudes $F_{\lambda\pm}(W,z)$ contains the partial-wave helicity amplitudes which may be analogously denoted as $f^j_{\lambda\pm}(W)$, with the same meaning of indices; note that $j \geq 1/2$ for $f^j_{1/2\pm}(W)$, while $j \geq 3/2$ for $f^j_{3/2\pm}(W)$.

Further, the helicity partial-wave amplitudes can be combined so to obtain two sets of definite-parity partial-wave amplitudes $f^{j\pm}_\lambda(W)$. According to Eq.(41) of Ref. [5], we obtain

$$\sqrt{2}\, f^{j\pm}_\lambda(W) = f^j_{\lambda+}(W) \pm \eta_\pi\eta_N\,(-1)^{j-1/2} f^j_{\lambda-}(W)\,, \tag{21}$$

where $\lambda = 1/2$ or $3/2$, the upper sign $\pm$ corresponds to the final (and initial as well) state parity equal to ±1, η_π and η_N are intrinsic parities of the pion and nucleon. The inverted expressions are

$$\sqrt{2}\, f^j_{\lambda+}(W) = f^{j+}_\lambda(E) + f^{j-}_\lambda(W)\,, \quad \sqrt{2}\,\eta_\pi\eta_N\,(-1)^{j-1/2} f^j_{\lambda-}(E) = f^{j+}_\lambda(W) - f^{j-}_\lambda(W)\,. \tag{22}$$

Of course, $\eta_\pi\eta_N = -1$, $(\eta_\pi\eta_N)^2 = 1$. Recall also that the lower sign + or − corresponds to the final state value $\mu = \pm1$, while the upper sign corresponds to parity of the final (and initial) state.

It is easy to check that

$$f^{j_1*}_{\lambda_1+}\, f^{j_2}_{\lambda_2+} \pm (-1)^{j_1+j_2+1} f^{j_1*}_{\lambda_1-}\, f^{j_2}_{\lambda_2-} = f^{j_1+*}_{\lambda_1}\, f^{j_2\pm}_{\lambda_2} + f^{j_1-*}_{\lambda_1}\, f^{j_2\mp}_{\lambda_2}\,, \tag{23}$$

$$(-1)^{j_2+1/2}\, f^{j_1*}_{\lambda_1+}\, f^{j_2}_{\lambda_2-} \pm (-1)^{j_1+1/2}\, f^{j_1*}_{\lambda_1-}\, f^{j_2}_{\lambda_2+} = f^{j_1\pm*}_{\lambda_1}\, f^{j_2+}_{\lambda_2} - f^{j_1\mp*}_{\lambda_1}\, f^{j_2-}_{\lambda_2}\,. \tag{24}$$

In particular,

$$|f^j_{\lambda+}|^2 + |f^j_{\lambda-}|^2 = |f^{j+}_\lambda|^2 + |f^{j-}_\lambda|^2\,, \quad |f^j_{\lambda+}|^2 - |f^j_{\lambda-}|^2 = 2\,\mathrm{Re}(f^{j+*}_\lambda\, f^{j-}_\lambda)$$

(recall that here all the j-values are half-integer, so $j_1 + j_2 + 1$ is always an integer). The translation from these partial-wave amplitudes to the helicity elements, $A_{\ell\pm}$ and $B_{\ell\pm}$, as well as the multipole amplitudes, $E_{\ell\pm}$ and $M_{\ell\pm}$, is given in Ref. [6]. For example, we have

$$-f^{1/2-}_{1/2} = A_{0+} = E_{0+}\ , \tag{25}$$

$$f^{1/2+}_{1/2} = A_{1-} = M_{1-}\ , \tag{26}$$

where the subscript notation $\ell\pm$ for helicity elements and multipoles [7] denotes a state with orbital angular momentum ℓ and total angular momentum $j = \ell \pm 1/2$.

The above analysis is equally applicable for the process of the η-meson photoproduction

$$\gamma + p \to \eta + p \tag{27}$$

(or for π^0 photoproduction). The energy region of η production, investigated experimentally in Ref. [1], is assumed to contain N^* resonances with spins up to 5/2 [8]. One can expect, therefore, that the decompositions should essentially run up to $j = 5/2$ in Eq.(3) and up to $J = 5$ in Eq.(9). Such an expectation agrees with the fit to data [1]: extracted

Legendre coefficients with $J > 5$ appear to be consistent with zero, within their uncertainties. The Wigner harmonics necessary for the amplitude decompositions are given explicitly in Appendix 1C. (Note that for the π^0 production, at similar energies [2, 3], one needs more lengthy decompositions up to $J = 10$, because of the lower associated threshold.)

Now we can illustrate our approach in more detail for the cross sections of the reaction (27). We use Eq.(8) (truncated up to $j_{1,2} = 5/2$) and decompositions of Appendix 1D to derive expressions for the Legendre coefficients $A_J^{(\sigma)}$ $(J = 0, ..., 5)$. They are shown in Appendix 2A. Note that $A_0^{(\sigma)}$ can be rewritten in the form

$$\frac{1}{2N}\, A_0^{(\sigma)}(W) = \sum_{j\geq 1/2} (2j+1)\, \left(|f_{1/2}^{j+}|^2 + |f_{1/2}^{j-}|^2 \right) + \sum_{j\geq 3/2} (2j+1)\, \left(|f_{3/2}^{j+}|^2 + |f_{3/2}^{j-}|^2 \right) ; \tag{28}$$

the left-hand side factor $1/2$ accounts for the fact that the right-hand side expression contains contributions of only one sign of the total helicities, $+1/2$ and $+3/2$, while $A_0^{(\sigma)}$ should contain also contributions with the negative sign of helicities (recall that positive and negative sign contributions are equal to each other, due to parity conservation). This relation is true even without j-truncating and clearly shows that $A_0^{(\sigma)}$ is indeed proportional to the total (*i.e.*, integrated differential) cross section, as it should be.

Explicit expressions of Appendix 2A confirm the properties of the Legendre coefficients formulated above. Every coefficient has two parts, corresponding to $\lambda = 1/2$ and $\lambda = 3/2$. Of course, states with $j = 1/2$ contribute only to $\lambda = 1/2$. Coefficients $A_J^{(\sigma)}$ with even J consist of proper contributions of various partial-wave states and interference contributions of states with different j, but with the same parities, both positive and negative. On the other hand, the odd-J coefficients contain only interferences between states of the same or different values of j, but always with opposite parities, exactly as stated in the preceding Section. As the value of J increases, so does the number of contributions to $A_J^{(\sigma)}$. The simple structure of $A_4^{(\sigma)}$ and $A_5^{(\sigma)}$ in Appendix 2 is the result of our assuming the absence of states with $j > 5/2$. In particular, it is because of this assumption that states with $j = 1/2$ are not seen in the displayed expressions for $A_4^{(\sigma)}$ and $A_5^{(\sigma)}$.

This approach can be easily applied to other polarization observables. For example, the double polarization observable $\check{E}(W, z) = E \cdot d\sigma/dz$ may also be expanded in Legendre polynomials $P_J(z)$, similar to Eq.(9), but with different Legendre coefficients $A_J^{(E)}(W)$. Comparison of expressions (19) and (20) shows that $A_J^{(\sigma)}(W)$ and $A_J^{(E)}(W)$ differ only in the sign of all contributions with $\lambda = 3/2$. The beam-polarizaton quantity, Σ, is also treated within the helicity formalism in Ref. [6],

$$\Sigma(W, z) \cdot \frac{d\sigma(W, z)}{dz} = 4N\, \mathrm{Re}\left[F_{1/2-}^{*}(W, z)\, F_{3/2+}(W, z) - F_{1/2+}^{*}(W, z)\, F_{3/2-}(W, z) \right] . \tag{29}$$

Both terms in the square brackets contain the kinematical edge factor $(1-z^2)$, and we expand them over the associated Legendre functions $P_J^2(z)$ with $J \geq 2$, which all have the same edge factor:

$$\hat{\Sigma}(W, z) \equiv \Sigma(W, z) \cdot \frac{d\sigma(W, z)}{dz} = \sum_{J=2}^{\infty} A_J^{(\Sigma)}(W)\, P_J^2(z) . \tag{30}$$

Application of property (12) to the right-hand side of expression (29) shows that the coefficients $A_J^{(\Sigma)}(W)$ also contain parity correlations, just in the same way as the coefficients $A_J^{(\sigma)}(W)$ for the unpolarized cross section.

Expansions for products of d-harmonics, up to $j = 5/2$, arising in Eq.(29) are given in Appendix 1E. They allow to obtain $A_J^{(\Sigma)}(W)$ with $J \leq 5$ truncated at $j = 5/2$. The results are shown in Appendix 2B. All contributions to the Legendre coefficients $A_J^{(\Sigma)}(W)$ come from interferences of amplitudes with initial total helicities $1/2$ and $3/2$. State parities are correlated exactly as for $A_J^{(\sigma)}(W)$: the same parities in the even-J coefficients and opposite parities in the odd-J ones. There is, however, an interesting difference, not quite evident in expression (29). Inversion of parities for all states does not change $A_J^{(\sigma)}(W)$ and, therefore, the cross sections (differential and total). On the other hand, such a transformation reverses the signs of all $A_J^{(\Sigma)}(W)$ and, therefore, of $\hat{\Sigma}(W, z)$ and $\Sigma(W, z)$ as well.

IV. APPLICATION TO DATA

The expansion method requires data of both high precision and broad angular coverage to determine the higher-order coefficients. A prime example is provided by the A2 Collaboration at MAMI which recently reported 7978

$d\sigma/d\Omega$ data for the reaction $\gamma p \to \pi^0 p$ and for for incident photon energies E from 218 to 1573 MeV (or for c.m energies W = 1136 – 1957 MeV) [2]. These data are obtained with a fine binning in E (∼4 MeV for all energies below E = 1120 MeV) and 30 angular bins, giving a good coverage of the π^0 production angle. The data obtained above E = 1443 MeV (W = 1894 MeV), however, have a limited angular coverage and for this reason were excluded from the present Legendre fit.

A good description of the $\gamma p \to \pi^0 p$ differential cross sections was obtained, for each included energy bin and the full angular range, in a fit with Legendre polynomials up to order ten (Eq.(9)) - the coefficients $A_J^{(\sigma)}$ depending on energy.

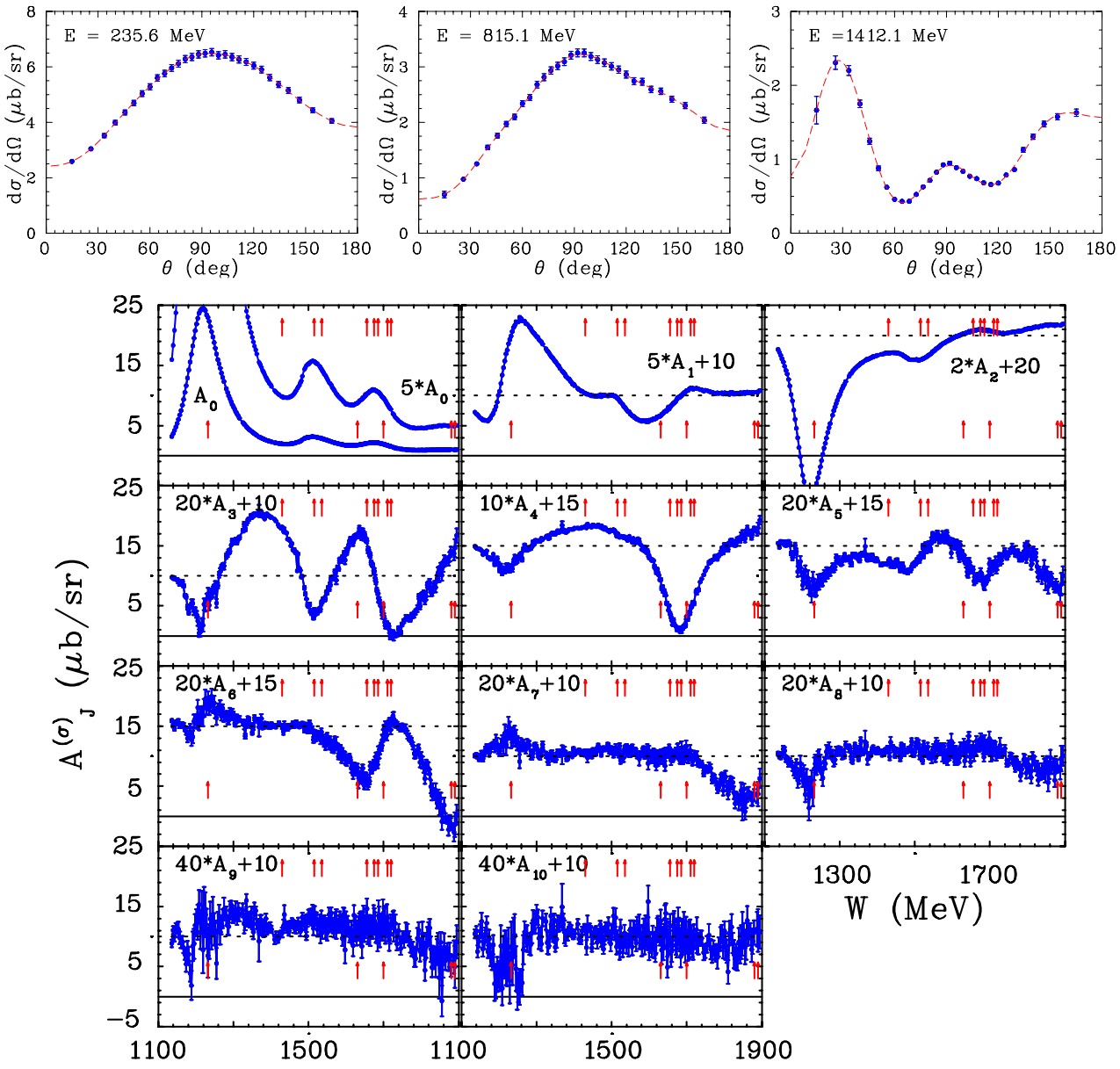

FIG. 1. (Color online) *Top panel*: Samples of the $\gamma p \to \pi^0 p$ differential cross sections, $d\sigma/d\Omega$, from A2 Collaboration at MAMI measurements (blue filled circles) [2] with the best fit results using Legendre polynomials (red dashed lines). The error bars on all data points represent statistical uncertaities only. Values of E in each plot indicate the lab photon energies. *Bottom panel*: Coefficients of Legendre polynomials (blue filled circles). The error bars of all values represent $A_J^{(\sigma)}$ uncertainties from the fits in which only the statistical uncertainties were used. Solid lines are plotted to help guide the eye. Red vertical arrows indicate masses of the four-star resonances (BW masses) known in this energy range [8]. The upper row of arrows corresponds to N^* states with isospin $I = 1/2$ and the lower row corresponds to Δ^* with $I = 3/2$.

The typical experimental statistics and the Legendre-polynomial fits are illustrated in Fig. 1(top panel) for different

energies. The results of the Legendre-polynomial fits for each coefficient $A_J^{(\sigma)}$ are depicted in Fig. 1(bottom panel), showing their energy dependence in unprecedented detail.

As expected from the form of Eq.(28), resonance contributions from the first, second and third resonance regions combine to produce clear peaks in the coefficient $A_0^{(\sigma)}$. These regions are somewhat less pronounced in $A_2^{(\sigma)}$, which also contains interference terms between states of the same parity. The result for $A_0^{(\sigma)}$ itself shows good agreement with the total cross section, obtained by an integration of the differential cross sections, confirming the quality of this dataset.

Other interesting features in Fig. 1, and the expanded plot of Fig. 2, are the sharp structures seen for each coefficient $A_J^{(\sigma)}$ in the region of $\Delta(1232)3/2^+$. This resonance can contribute directly (without interference) only to $A_0^{(\sigma)}$ and $A_2^{(\sigma)}$. Since there exists no other nearby resonance, such structures can appear only due to the interference of $\Delta(1232)3/2^+$ with other non-resonant partial-waves. Coefficient $A_1^{(\sigma)}$ should reveal the interference of $\Delta(1232)3/2^+$ with the three states having $J^P = 1/2^-$, $3/2^-$, and $5/2^-$. Higher coefficients $A_J^{(\sigma)}$ could reveal interference with the four states having $J = j - 3/2, j - 1/2, j + 1/2$, and $j + 3/2$, with parity positive for even j and negative for odd j. Thus, via such interference effects, the contributions from very high partial-wave amplitudes could be studied, a possibility not available in any other standard approach. This feature is similar to enhancing the manifestation of rare decay modes of resonances via the interference with other strong resonances [9].

It should be noted that the recurring sharp structures associated with the $\Delta(1232)$ energy region do not appear in multipole analyses of these data. The angle-independent systematic error was used to determine renormalization factors for each angular distribution. These factors were determined to be very near unity (within 1%) and, if applied to the data, had no effect on the higher Legendre coefficients. If instead, the statistical and systematic errors are added in quadrature [10], structures in the highest coefficients are masked by greatly expanded errors. This result emphasizes the importance of systematic error analysis, the effect of which may also be magnified by a dominant resonance.

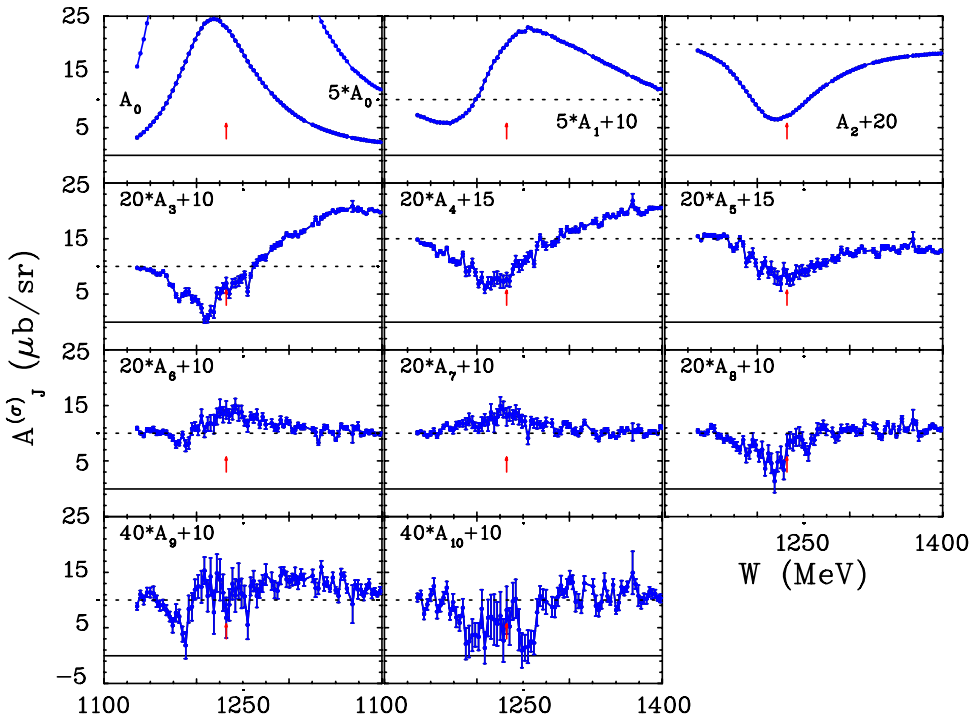

FIG. 2. (Color online) Zoom for A2 $\gamma p \to \pi^0 p$ data below W = 1400 MeV to cover the Δ-isobar region [2] as shown on Fig. 1(bottom panel).

The A2 collaboration at MAMI has also measured 2400 $d\sigma/d\Omega$s for the reaction $\gamma p \to \eta p$ and for for incident photon energies E from 710 and up to 1395 MeV (or for c.m energies W = 1488 – 1870 MeV] [1]. The large number of events accumulated allowed the division of the data into 120 bins in E. From the reaction threshold to an E of 1008 MeV, the bin width was that of a single tagger channel ($\sim$4 MeV). From 1008 to 1238 MeV, two tagger channels were combined to a single energy bin. Above 1238 MeV, an energy bin included from three to eight tagger channels. The $\gamma p \to \eta p$ differential cross sections were determined as a function of z. The z spectra at all energies were divided

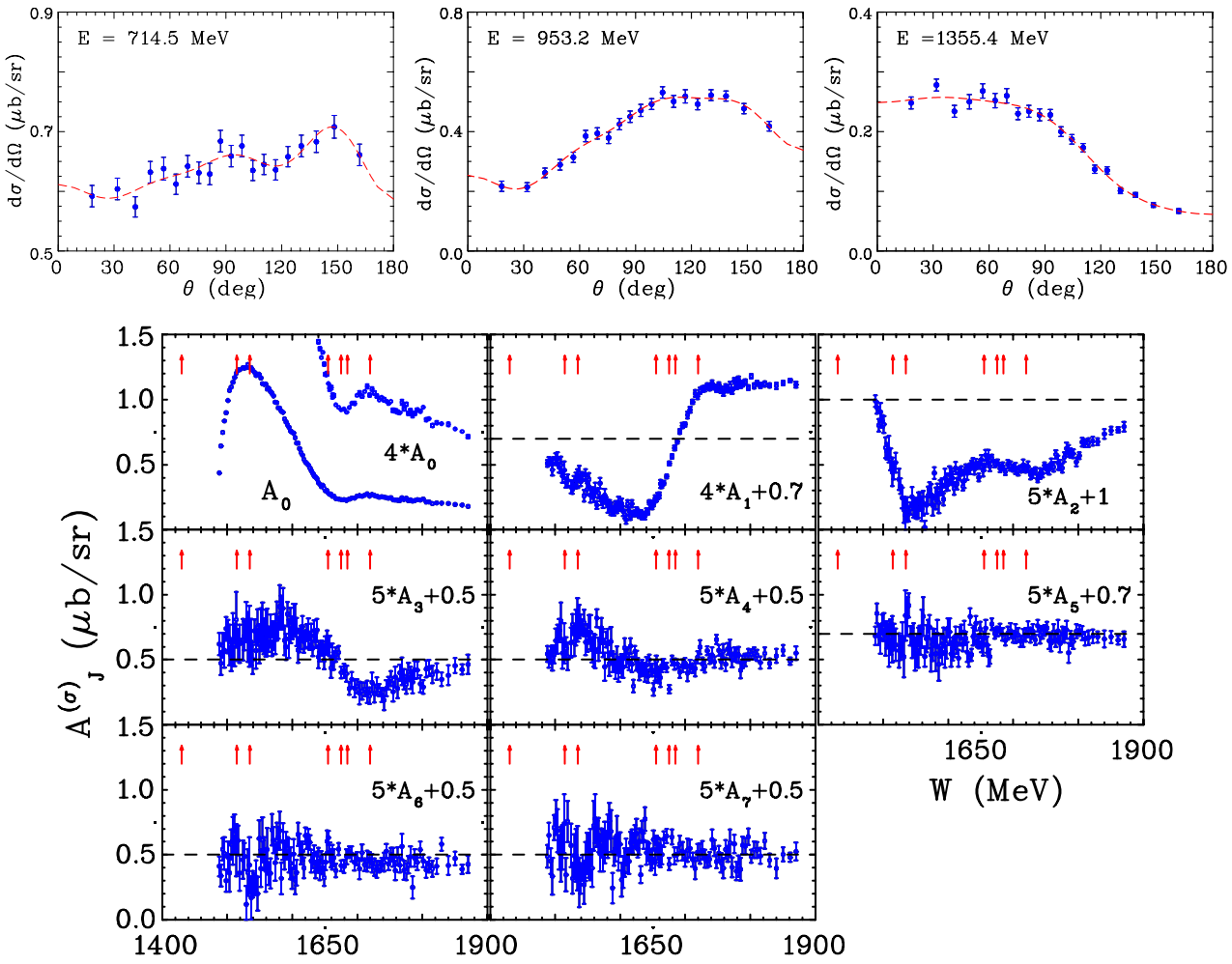

FIG. 3. (Color online) *Top panel*: Samples of the $\gamma p \to \eta p$ differential cross sections, $d\sigma/d\Omega$, from A2 Collaboration at MAMI measurements [1] with the best fit results using Legendre polynomials. The notation as given in Fig. 1. *Bottom panel*: Coefficients for Legendre polynomials. The notation is given in Fig. 1.

into 20 bins.

The photoproduction of eta mesons is interesting in that only isospin 1/2 resonances can contribute, thus reducing the list of candidates required to explain energy-dependent structures in the Legendre coefficients. For many N^* states, the decay to ηN has been determined to be very weak. This too helps in deciphering the sources of structures.

In Fig. 3(top panel), differential cross sections for three incident photon energies are compared with the Legendre-polynomial fits. The results of the Legendre-polynomial fits for each coefficient $A_J^{(\sigma)}$ are depicted in Fig. 3(bottom panel), showing their energy dependence. The full angular coverage of A2 differential cross sections together with small statistical uncertainties allowed a reliable determination of several Legendre coefficients $A_J^{(\sigma)}$, which was difficult to achieve with the previous data.

The behavior of these Legendre coefficients suggests possible resonance contributions, though some puzzles remain. Unlike the pion photoproduction case, $A_0^{(\sigma)}$ reveals only one dominant resonance (N(1535)$1/2^-$) with a small shoulder near 1700 MeV, possibly containing several states. While the $\Delta(1232)$ state appeared prominently also in $A_2^{(\sigma)}$, the lower-spin N(1535) does not. Instead, near threshold there is a nearly linear drop from zero, which must involve an interference with the dominant N(1535). From Appendix 2, likely states have $J^P = 3/2^-$ and $5/2^-$.

Perhaps the most intriguing structure is seen in $A_1^{(\sigma)}$. Assuming this is due to states, with opposite parity, interfering with the tail of the dominant N(1535), candidates include $J^P = 1/2^+$ and $3/2^+$. The crossover seen, less clearly, in the coefficient $A_3^{(\sigma)}$ nearly mirrors that found in $A_1^{(\sigma)}$, suggesting a common origin.

V. DISCUSSION AND CONCLUSIONS

Several examples of the Legendre analyses, discussed in this paper, are rather simple. They, nevertheless, allow us to demonstrate various features, inherent also in more general and complicated cases. That is why we are now able to formulate a number of sufficiently general conclusions.

- Legendre expansions provide a model-independent approach suitable for presentation of modern detailed (high-precision and high-statistics) data for two-hadron reactions.
- This approach is applicable both to cross sections and to polarization variables; it is much more compact than traditional methods, at least, at energies within the resonance region.
- The Legendre coefficients reveal specific correlations and interferences between states of definite parities.
- Due to interference with resonances, high-momentum Legendre coefficients open a window to study higher partial-wave amplitudes, which are out-of-reach within any other method.

Concluding this brief discussion, one should emphasize that direct interference has become a useful instrument to search for and study rare decays of well-established resonances. However, its possibilities are limited by restrictions for the resonance quantum numbers. Rescattering interference is not limited by such requirements and, therefore, may provide effective methods to search for and study new resonances with arbitrary quantum numbers. Data on multi-hadron decays of heavy particles also present a new rapidly-expanding area for applications of different kinds of interference both to study spectroscopy of resonances and to establish their characteristics.

Acknowledgments

Ya. I. A. acknowledged support by the Russian Science Foundation (Grant No. 14–22–00281); the work of W. J. B. and I. I. S. is supported, in part, by the U. S. Department of Energy, Office of Science, Office of Nuclear Physics, under Awards No. de–sc0014133 and de–sc0016583. R. L. W. is supported by the U. S. Department of Energy Grant de–sc0016582.

Appendix 1. Wigner harmonics and Legendre functions

For convenience, here we give explicitly those Legendre functions and Wigner harmonics which can be used to describe differential cross sections and beam asymmetries for reactions (15) and (27) up to $j, J = 5$.

A) Legendre functions $P_J(z)$ with $J \le 5$:

$$P_0(z) = 1, \quad P_1(z) = z, \quad P_2(z) = \frac{1}{2}(3z^2 - 1), \quad P_3(z) = \frac{1}{2}(5z^3 - 3z),$$

$$P_4(z) = \frac{1}{8}(35z^4 - 30z^2 + 3), \quad P_5(z) = \frac{1}{8}(63z^5 - 70z^3 + 15z)\,.$$

B) Associated Legendre functions $P_J^2(z)$ with $J \le 5$:

$$\frac{P_2^2(z)}{(1-z^2)} = 3, \quad \frac{P_3^2(z)}{(1-z^2)} = 15z, \quad \frac{P_4^2(z)}{(1-z^2)} = \frac{15}{2}(7z^2 - 1), \quad \frac{P_5^2(z)}{(1-z^2)} = \frac{105z}{2}(3z^2 - 1)\,.$$

C) Wigner harmonics $d^j_{\lambda,\mu}(z)$ with $j \le 5/2$ for $\lambda = \pm 3/2, \pm 1/2$ and $\mu = \pm 1/2$.

$$d^j_{-1/2,-1/2}(z) = d^j_{1/2,1/2}(z)\,, \qquad d^j_{-1/2,1/2}(z) = -d^j_{1/2,-1/2}(z) = (-1)^{j-1/2}\, d^j_{1/2,1/2}(-z)\,,$$

$$d^j_{-3/2,-1/2}(z) = -d^j_{3/2,1/2}(z)\,, \quad d^j_{-3/2,1/2}(z) = d^j_{3/2,-1/2}(z) = (-1)^{j-1/2}\, d^j_{3/2,1/2}(-z)\,.$$

It is sufficient, therefore, to know explicitly only d-functions with both λ and μ positive. a) The case of $\lambda = 1/2$:

$$d^{1/2}_{1/2,1/2}(z) = \sqrt{\frac{1+z}{2}}\,, \quad d^{3/2}_{1/2,1/2}(z) = \frac{1}{2}\sqrt{\frac{1+z}{2}}\,(3z-1)\,, \quad d^{5/2}_{1/2,1/2}(z) = \frac{1}{2}\sqrt{\frac{1+z}{2}}\,(5z^2 - 2z - 1)\,.$$

b) The case of $\lambda = 3/2$:

$$d^{3/2}_{3/2,1/2}(z) = -\frac{\sqrt{3}}{2}\sqrt{\frac{1-z}{2}}\,(1+z)\,, \quad d^{5/2}_{3/2,1/2}(z) = -\frac{\sqrt{2}}{4}\sqrt{\frac{1-z}{2}}\,(1+z)(5z-1)\,.$$

D) Expansions (for cross sections) over Legendre functions.

a) Quadratic terms with $\lambda = 1/2$:

$$[\,d^{1/2}_{1/2,1/2}(z)\,]^2 = \frac{1}{2}\,P_1(z) + \frac{1}{2}\,P_0(z)\,,$$

$$[\,d^{3/2}_{1/2,1/2}(z)\,]^2 = \frac{9}{20}\,P_3(z) + \frac{1}{4}\,P_2(z) + \frac{1}{20}\,P_1(z) + \frac{1}{4}\,P_0(z)\,,$$

$$[\,d^{5/2}_{1/2,1/2}(z)\,]^2 = \frac{25}{63}\,P_5(z) + \frac{1}{7}\,P_4(z) + \frac{4}{45}\,P_3(z) + \frac{4}{21}\,P_2(z) + \frac{1}{70}\,P_1(z) + \frac{1}{6}\,P_0(z)\,,$$

$$[\,d^{j}_{1/2,-1/2}(z)\,]^2 = [\,d^{j}_{1/2,1/2}(-z)\,]^2\,.$$

b) Bilinear terms with different j, the same $\lambda = 1/2$, and $\mu = \pm 1/2$:

$$d^{1/2}_{1/2,1/2}(z)\,d^{3/2}_{1/2,1/2}(z) = \frac{1}{2}\,P_2(z) + \frac{1}{2}\,P_1(z)\,, \quad d^{1/2}_{1/2,1/2}(z)\,d^{5/2}_{1/2,1/2}(z) = \frac{1}{2}\,P_3(z) + \frac{1}{2}\,P_2(z)\,,$$

$$d^{3/2}_{1/2,1/2}(z)\,d^{5/2}_{1/2,1/2}(z) = \frac{3}{7}\,P_4(z) + \frac{1}{5}\,P_3(z) + \frac{1}{14}\,P_2(z) + \frac{3}{10}\,P_1(z)\,,$$

$$d^{j_1}_{1/2,-1/2}(z)\,d^{j_2}_{1/2,-1/2}(z) = (-1)^{j_1+j_2-1}\,d^{j_1}_{1/2,1/2}(-z)\,d^{j_2}_{1/2,1/2}(-z)\,.$$

c) Quadratic terms with $\lambda = 3/2$:

$$[\,d^{3/2}_{3/2,1/2}(z)\,]^2 = -\frac{3}{20}\,P_3(z) - \frac{1}{4}\,P_2(z) + \frac{3}{20}\,P_1(z) + \frac{1}{4}\,P_0(z)\,,$$

$$[\,d^{5/2}_{3/2,1/2}(z)\,]^2 = -\frac{25}{126}\,P_5(z) - \frac{3}{14}\,P_4(z) + \frac{7}{45}\,P_3(z) + \frac{1}{21}\,P_2(z) + \frac{3}{70}\,P_1(z) + \frac{1}{6}\,P_0(z)\,,$$

$$[\,d^{j}_{3/2,-1/2}(z)\,]^2 = [\,d^{j}_{3/2,1/2}(-z)\,]^2\,.$$

d) Bilinear terms with different j, the same $\lambda = 3/2$, and $\mu = \pm 1/2$:

$$d^{3/2}_{3/2,1/2}(z)\,d^{5/2}_{3/2,1/2}(z) = \sqrt{\frac{3}{2}}\,\left[-\frac{1}{7}\,P_4(z) - \frac{1}{5}\,P_3(z) + \frac{1}{7}\,P_2(z) + \frac{1}{5}\,P_1(z)\right]\,,$$

$$d^{j_1}_{3/2,-1/2}(z)\,d^{j_2}_{3/2,-1/2}(z) = (-1)^{j_1+j_2-1}\,d^{j_1}_{3/2,1/2}(-z)\,d^{j_2}_{3/2,1/2}(-z)\,.$$

E) Expansions (for beam asymmetry) over associated Legendre functions:

$$d^{1/2}_{1/2,-1/2}(z)\,d^{3/2}_{3/2,1/2}(z) = \frac{\sqrt{3}}{12}\,P^2_2(z)\,, \quad d^{1/2}_{1/2,-1/2}(z)\,d^{5/2}_{3/2,1/2}(z) = \frac{\sqrt{2}}{24}\,\left[P^2_3(z) - P^2_2(z)\right]\,,$$

$$d^{3/2}_{1/2,-1/2}(z)\,d^{3/2}_{3/2,1/2}(z) = \frac{\sqrt{3}}{8}\,\left[\frac{1}{5}\,P^2_3(z) + \frac{1}{3}\,P^2_2(z)\right]\,,$$

$$d^{3/2}_{1/2,-1/2}(z)\, d^{5/2}_{3/2,1/2}(z) = \frac{\sqrt{2}}{8}\left[\frac{1}{7}\,P^2_4(z) + \frac{1}{15}\,P^2_3(z) + \frac{4}{21}\,P^2_2(z)\right],$$

$$d^{5/2}_{1/2,-1/2}(z)\, d^{3/2}_{3/2,1/2}(z) = \frac{\sqrt{3}}{12}\left[\frac{1}{7}\,P^2_4(z) + \frac{1}{5}\,P^2_3(z) - \frac{1}{7}\,P^2_2(z)\right],$$

$$d^{5/2}_{1/2,-1/2}(z)\, d^{5/2}_{3/2,1/2}(z) = \frac{\sqrt{2}}{16}\left[\frac{10}{63}\,P^2_5(z) + \frac{2}{21}\,P^2_4(z) + \frac{4}{45}\,P^2_3(z) + \frac{4}{7}\,P^2_2(z)\right],$$

$$d^{j_1}_{1/2,1/2}(z)\, d^{j_2}_{3/2,-1/2}(z) = (-1)^{j_1+j_2}\, d^{j_1}_{1/2,-1/2}(-z)\, d^{j_2}_{3/2,1/2}(-z)\,, \quad P^2_J(-z) = (-1)^J\, P^2_J(z)\,.$$

Appendix 2. Legendre coefficients

A) Coefficients for cross section.

a) Even values of J:

$$\frac{1}{2N}\,A^{(\sigma)}_0(E) = 2\left(|f^{1/2+}_{1/2}|^2 + |f^{1/2-}_{1/2}|^2\right) + 4\left(|f^{3/2+}_{1/2}|^2 + |f^{3/2-}_{1/2}|^2\right) + 6\left(|f^{5/2+}_{1/2}|^2 + |f^{5/2-}_{1/2}|^2\right)$$

$$+4\left(|f^{3/2+}_{3/2}|^2 + |f^{3/2-}_{3/2}|^2\right) + 6\left(|f^{5/2+}_{3/2}|^2 + |f^{5/2-}_{3/2}|^2\right);$$

$$\frac{1}{2N}\,A^{(\sigma)}_2(E) = 4\left(|f^{3/2+}_{1/2}|^2 + |f^{3/2-}_{1/2}|^2\right) + \frac{48}{7}\left(|f^{5/2+}_{1/2}|^2 + |f^{5/2-}_{1/2}|^2\right)$$

$$+ 8\,\mathrm{Re}\left(f^{1/2+*}_{1/2} f^{3/2+}_{1/2} + f^{1/2-*}_{1/2} f^{3/2-}_{1/2}\right) + 12\,\mathrm{Re}\left(f^{1/2+*}_{1/2} f^{5/2+}_{1/2} + f^{1/2-*}_{1/2} f^{5/2-}_{1/2}\right)$$

$$+ \frac{24}{7}\,\mathrm{Re}\left(f^{3/2+*}_{1/2} f^{5/2+}_{1/2} + f^{3/2-*}_{1/2} f^{5/2-}_{1/2}\right) - 4\left(|f^{3/2+}_{3/2}|^2 + |f^{3/2-}_{3/2}|^2\right)$$

$$+ \frac{12}{7}\left(|f^{5/2+}_{3/2}|^2 + |f^{5/2-}_{3/2}|^2\right) + \frac{24}{7}\sqrt{6}\,\mathrm{Re}\left(f^{3/2+*}_{3/2} f^{5/2+}_{3/2} + f^{3/2-*}_{3/2} f^{5/2-}_{3/2}\right);$$

$$\frac{1}{2N}\,A^{(\sigma)}_4(E) = \frac{36}{7}\left(|f^{5/2+}_{1/2}|^2 + |f^{5/2-}_{1/2}|^2\right) + \frac{144}{7}\,\mathrm{Re}\left(f^{3/2+*}_{1/2} f^{5/2+}_{1/2} + f^{3/2-*}_{1/2} f^{5/2-}_{1/2}\right)$$

$$- \frac{108}{7}\left(|f^{5/2+}_{3/2}|^2 + |f^{5/2-}_{3/2}|^2\right) - \frac{24}{7}\sqrt{6}\,\mathrm{Re}\left(f^{3/2+*}_{3/2} f^{5/2+}_{3/2} + f^{3/2-*}_{3/2} f^{5/2-}_{3/2}\right).$$

b) Odd values of J:

$$\frac{1}{2N}\,A^{(\sigma)}_1(E) = 4\,\mathrm{Re}\left(f^{1/2+*}_{1/2} f^{1/2-}_{1/2}\right) + \frac{8}{5}\,\mathrm{Re}\left(f^{3/2+*}_{1/2} f^{3/2-}_{1/2}\right) + \frac{36}{35}\,\mathrm{Re}\left(f^{5/2+*}_{1/2} f^{5/2-}_{1/2}\right)$$

$$+8\,\mathrm{Re}\left(f^{1/2+*}_{1/2} f^{3/2-}_{1/2} + f^{1/2-*}_{1/2} f^{3/2+}_{1/2}\right) + \frac{72}{5}\,\mathrm{Re}\left(f^{3/2+*}_{1/2} f^{5/2-}_{1/2} + f^{3/2-*}_{1/2} f^{5/2+}_{1/2}\right)$$

$$+ \frac{24}{5}\,\mathrm{Re}\left(f^{3/2+*}_{3/2} f^{3/2-}_{3/2}\right) + \frac{108}{35}\,\mathrm{Re}\left(f^{5/2+*}_{3/2} f^{5/2-}_{3/2}\right) + \frac{24}{5}\sqrt{6}\,\mathrm{Re}\left(f^{3/2+*}_{3/2} f^{5/2-}_{3/2} + f^{3/2-*}_{3/2} f^{5/2+}_{3/2}\right);$$

$$\frac{1}{2N}\,A^{(\sigma)}_3(E) = \frac{72}{5}\,\mathrm{Re}\left(f^{3/2+*}_{1/2} f^{3/2-}_{1/2}\right) + \frac{32}{5}\,\mathrm{Re}\left(f^{5/2+*}_{1/2} f^{5/2-}_{1/2}\right) + 12\,\mathrm{Re}\left(f^{1/2+*}_{1/2} f^{5/2-}_{1/2} + f^{1/2-*}_{1/2} f^{5/2+}_{1/2}\right)$$

$$+\frac{48}{5}\,\mathrm{Re}\left(f_{1/2}^{3/2+*}f_{1/2}^{5/2-}+f_{1/2}^{3/2-*}f_{1/2}^{5/2+}\right)-\frac{24}{5}\,\mathrm{Re}\left(f_{3/2}^{3/2+*}f_{3/2}^{3/2-}\right)+\frac{56}{5}\,\mathrm{Re}\left(f_{3/2}^{5/2+*}f_{3/2}^{5/2-}\right)$$

$$-\frac{24}{5}\sqrt{6}\,\mathrm{Re}\left(f_{3/2}^{3/2+*}f_{3/2}^{5/2-}+f_{3/2}^{3/2-*}f_{3/2}^{5/2+}\right);$$

$$\frac{1}{2N}\,A_5^{(\sigma)}(E)=\frac{200}{7}\,\mathrm{Re}\left(f_{1/2}^{5/2+*}f_{1/2}^{5/2-}\right)-\frac{100}{7}\,\mathrm{Re}\left(f_{3/2}^{5/2+*}f_{3/2}^{5/2-}\right).$$

B) Coefficients for beam asymmetry.
a) Even values of J:

$$\frac{1}{4N}\,A_2^{(\Sigma)}(E)=\frac{2}{3}\sqrt{3}\,\mathrm{Re}\left(f_{1/2}^{1/2-*}f_{3/2}^{3/2-}-f_{1/2}^{1/2+*}f_{3/2}^{3/2+}\right)-\frac{\sqrt{2}}{2}\,\mathrm{Re}\left(f_{1/2}^{1/2-*}f_{1/2}^{5/2-}-f_{1/2}^{1/2+*}f_{1/2}^{5/2+}\right)$$

$$-\frac{2}{3}\sqrt{3}\,\mathrm{Re}\left(f_{1/2}^{3/2-*}f_{3/2}^{3/2-}-f_{1/2}^{3/2+*}f_{3/2}^{3/2+}\right)-\frac{2}{7}\sqrt{2}\,\mathrm{Re}\left(f_{1/2}^{3/2-*}f_{3/2}^{5/2-}-f_{1/2}^{3/2+*}f_{3/2}^{5/2+}\right)$$

$$-\frac{2}{7}\sqrt{3}\,\mathrm{Re}\left(f_{1/2}^{5/2-*}f_{3/2}^{3/2-}-f_{1/2}^{5/2+*}f_{3/2}^{3/2+}\right)+\frac{9}{7}\sqrt{2}\,\mathrm{Re}\left(f_{1/2}^{5/2-*}f_{3/2}^{5/2-}-f_{1/2}^{5/2+*}f_{3/2}^{5/2+}\right);$$

$$\frac{1}{4N}\,A_4^{(\Sigma)}(E)=-\frac{3}{14}\sqrt{2}\,\mathrm{Re}\left(f_{1/2}^{3/2-*}f_{3/2}^{5/2-}-f_{1/2}^{3/2+*}f_{3/2}^{5/2+}\right)-\frac{2}{7}\sqrt{3}\,\mathrm{Re}\left(f_{1/2}^{5/2-*}f_{3/2}^{3/2-}-f_{1/2}^{5/2+*}f_{3/2}^{3/2+}\right)$$

$$+\frac{3}{14}\sqrt{2}\,\mathrm{Re}\left(f_{1/2}^{5/2-*}f_{3/2}^{5/2-}-f_{1/2}^{5/2+*}f_{3/2}^{5/2+}\right).$$

b) Odd values of J:

$$\frac{1}{4N}\,A_3^{(\Sigma)}(E)=\frac{\sqrt{2}}{2}\,\mathrm{Re}\left(f_{1/2}^{1/2-*}f_{3/2}^{5/2+}-f_{1/2}^{1/2+*}f_{3/2}^{5/2+}\right)-\frac{2}{5}\sqrt{3}\,\mathrm{Re}\left(f_{1/2}^{3/2-*}f_{3/2}^{3/2+}-f_{1/2}^{3/2+*}f_{3/2}^{3/2-}\right)$$

$$-\frac{\sqrt{2}}{10}\,\mathrm{Re}\left(f_{1/2}^{3/2-*}f_{1/2}^{5/2+}-f_{1/2}^{3/2+*}f_{1/2}^{5/2-}\right)+\frac{2}{5}\sqrt{3}\,\mathrm{Re}\left(f_{1/2}^{5/2-*}f_{3/2}^{3/2+}-f_{1/2}^{5/2+*}f_{3/2}^{3/2-}\right)$$

$$+\frac{1}{5}\sqrt{2}\,\mathrm{Re}\left(f_{1/2}^{5/2-*}f_{3/2}^{5/2+}-f_{1/2}^{5/2+*}f_{3/2}^{5/2-}\right);$$

$$\frac{1}{4N}\,A_5^{(\Sigma)}(E)=\frac{5}{14}\sqrt{2}\,\mathrm{Re}\left(f_{1/2}^{5/2-*}f_{3/2}^{5/2+}-f_{1/2}^{5/2+*}f_{3/2}^{5/2-}\right).$$

[1] E. F. McNicoll *et al.* (Crystal Ball Collaboration at MAMI), Phys. Rev. C **82**, 035208 (2010); arXiv:1007.0777 [nucl–ex].
[2] P. Adlarson *et al.* (A2 Collaboration at MAMI), Phys. Rev. C **92**, 024617 (2015); arXiv:1506.08849 [hep–ex].
[3] M. Dugger *et al.* (CLAS Collaboration), Phys. Rev. C **88**, 065203 (2013); arXiv:1308.4028 [nucl–ex].
[4] Ya. Azimov, to be published in Nucl. Phys. B - Proceedings Supplements, *Hadron Structure and QCD: from Low to High Energies* (HSQCD16), Gatchina, Russia, June-July, 2016; arXiv:1610.09677 [hep–ph].
[5] M. Jacob and G. C. Wick, Annals of Phys. **7**, 404 (1959).
[6] R. L. Walker, **182**, 1729 (1969).
[7] G. F. Chew, M. L. Goldberger, F. E. Low, and Y. Nambu, Phys. Rev. **106**, 1345 (1957).
[8] C. Patrignan *et al.* (Particle Data Group), Chin. Phys. C **40**, 100001 (2016).
[9] Ya. Azimov, J. Phys. G **37**, 023001 (2010); arXiv:0904.1376 [hep–ph].
[10] Y. Wunderlich, F. Afzal, A. Thiel, and R. Beck, arXiv:1611.01031 [nucl–ex].